HEFAT2014
10th International Conference on Heat Transfer, Fluid Mechanics and Thermodynamics
14 – 16 July 2014
Orlando, Florida

SURGE CONTROL OF AIR COMPRESSOR UNDER VARIABLE OPERATING PRESSURE OF AUTOMOTIVE FUEL CELLS

Jaeyoung Han and Sangseok Yu*
Department of Mechanical Engineering,
National University of Chungnam,
Daejon, 305-764,
Korea,
E-mail: sangseok@cnu.ac.kr

ABSTRACT

The compressor of a proton exchange membrane fuel cell for automotive application requires severe dynamic performance under normal operating conditions. Since the air flow rate with a compressor should cover a wide range of operating conditions, it is necessary to understand the operating trajectory of the compressor. In this study, a simulation model of an automotive fuel cell system with a dynamic compressor is developed to explore the proper trajectory of the air flow rate on the performance chart of an air compressor. A dynamic simulation model of a compressor is composed of manifold dynamics of a supply and return line, static compressor model, and dynamic motor model. From the compressor to the fuel cell stack is considered as a plenum and an orifice between them is also assumed. An active control valve is also considered at the exit of fuel cell stack so that the surge can be actively rejected. The control strategy of a variable pressure compressor is concentrated on rejection of surge over various operating conditions under the load demands of driving mode.

INTRODUCTION

The centrifugal compressor is widely used from the internal combustion engine to the energy industry, to pressurize air flows. In the case of the automotive fuel cell, the centrifugal compressor is responsible for supplying pressurized air to the fuel cell stack. High pressure operation of a fuel cell stack improves the performance and compact the packaging space for the system. When fuel cells are equipped in automobiles, SUVs are the typical application. However, since the sedan is a target of automotive fuel cell system, variable pressure operation is required to improve the performance with compact stacking [1].

A Surge is an unstable operating mode of compressor systems that occurs at low mass flow where the pressure delivered by the compressor is less than the plenum pressure [2]. As a compressor is operated under a dynamic environment, compressor surge can occur. The surge can damage the compressor, and the durability of whole system is difficult ensure. Since automotive fuel cells must be operated at a wide range of pressures, the compressor of the fuel cell must avoid the surges phenomenon.

NOMENCLATURE

ψ	[-]	Head parameter
U	[m/s]	Blade tip speed
Φ	[-]	The normalized compressor flow rate
ρ	[kg/m^3]	density
W	[kg/s]	Air mass flow rate
R	[J/molK]	Gas constant
T	[K]	Temperature
p	[pa]	Pressure
M	[-]	Mach number
d	[m]	diameter
A	[m^2]	Nozzle area
V	[V]	Stack voltage
P	[kW]	Stack power

Special characters

α	[-]	Reference coefficient at supply manifold
λ	[-]	Water content of H_2O/SO^{-3}
$\mathcal{B}$	[-]	Reference coefficient at cathode manifold
η	[V]	Cathode over-potential
γ	[-]	Ratio of specific heat

Subscripts

cp,in	Compressor in
cp,out	Compressor out
cp	compressor
a	Air
cr	Air mass flow of compressor
max	Maximum
0	Compressor inlet pressure
1	Compressor outlet pressure
sm,out	Supply manifold out
sm	Supply manifold
Nern	Nernst
FC	Fuel cell
ca	Cathode manifold
Ca,out	Cathode manifold out
ca	Cathode manifold

Surge control technology has been widely studied. Specifically, Greitzer et al. reported the dynamic characteristics of the entire axial load compression system of rotating stall and surge by theoretical and experimental research [2,3]. Moore & Greitzer proposed a surge model for a multistage axial load compression system [4]. Then Hansen et al. reported a model in 1981 based on one centrifugal compressor [5]. Shehata et al. reported an improved version of the Moore & Greitzer model for a centrifugal compressor [6]. They suggested several control techniques to avoid surges and consequently improve the efficiency of the system [6]. Also, Galindo et al. reported the experimental study of a centrifugal compressor of a turbocharger in small internal combustion engines [7]. Tirnovan, Miraoui and Giurgea present a study of fuel cell system performance operating at high pressure and different temperature levels [8].

In this study, a dynamic compressor model is developed that can simulate the compressor surge under a dynamic load follow-up of an automotive fuel cell system. The model is used to develop a surge rejection strategy of automotive fuel cells with the two valves for the supply manifold outlet and cathode out manifold. The efficiency and performance of the system is then discussed in terms of the combination of inlet and outlet valves of the fuel cell.

A DYNAMIC MODEL OF THE COMPRESSOR

Connection of thermodynamics with actual compressor map

In the present study, an Allied Signal compressor is used in the modeling of the compressor to determine the active control of surge. The model includes not only thermodynamic variable changes but also practical operating variables. The compressor model is divided into two parts: (1) a compressor air flow rate in the actual compressor (this is determined by the pressure ratio) and (2) the rotational speed of the compressor. Accordingly, the performance curve indicates the variation of air flow rates in terms of the pressure ratio and rotational speed of the compressor. As the inlet temperature of pressure affects the exit condition of the compressor, the performance curve of the compressor reflects the changes of the temperature and pressure such as modified flow rate, speed, and temperature. To normalize the performance curve, this study employs the normalized charge proposed by Jensen & Kristensen [10]. The non-dimension head parameter is as follows:

$$\Psi = \frac{C_p T_{cp,in}\left[\left(\frac{p_{cp,out}}{p_{cp,in}}\right)^{\frac{\gamma-1}{\gamma}} - 1\right]}{\frac{1}{2}U_c^2} \quad (1)$$

Where, U_c^2 is the compressor blade tip speeds.

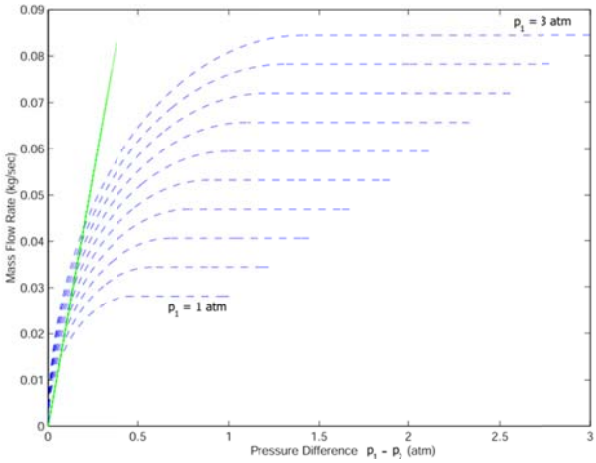

Figure 1 Comparison of nozzle flow rate

There, the normalized compressor flow rate (Φ) is then correlated with the head parameter (Ψ) by the following equation.

$$\Phi = \Phi_{\max}\left(1 - \exp^{\beta\left(\frac{\Psi}{\Psi_{\max}}-1\right)}\right) \quad (2)$$

Where, $\Phi_{\max}, \beta$ and $\Psi_{\max}$ are polynomial functions of the Mach number (M).

Therefore, the air mass flow is then calculated using Equation (3)

$$W_{cr} = \Phi \rho_a \frac{\pi}{4} d_c^2 U_c \quad (3)$$

Nozzle Equation

A nozzle is a device characteristic of a fluid flow as it exits an enclosed chamber or pipe to increase velocity. To develop the dynamic manifolds (inlet and outlet), this study utilizes the nozzle flow equation. The nozzle flow equation is applied to internal combustion engine fundamentals [9]. The air flow rate is a function of the upstream pressure p_0 and temperature T_1, and the downstream pressure p_1 of the nozzle.

$$\dot{W} = \frac{C_D A_R p_o}{(RT_o)^{1/2}}\left(\frac{p_1}{p_0}\right)^{1/\gamma}\left\{\frac{2\gamma}{\gamma-1}\left[1-\left(\frac{p_1}{p_0}\right)^{(\gamma-1)/\gamma}\right]\right\}^{1/2} \quad (4)$$

If the air flow rate ($\dot{W}$) through a nozzle is zero, the critical pressure ratio is calculated from the following.

$$\frac{p_1}{p_0} = \frac{2}{\gamma+1}^{\gamma/(\gamma-1)} \quad (0.528) \quad (5)$$

When the pressure drop is less than the critical pressure ratio, the appropriate equation is

$$\dot{W} = \frac{C_D A_R p_0}{(RT_o)^{1/2}} \gamma^{1/2} \left(\frac{2}{\gamma+1} \right)^{\gamma+1/2(\gamma-1)} \quad (6)$$

The plot of mass flow rate is shown in Fig.1. If the pressure difference between p_1 and p_2 is relatively small, the mass flow rate is equal for various manifold pressures due to Equation (4) ~ (6). Therefore, a small mass flow rate region can be calculated by a linearized form of Equation (4):

$$W = k(p_1 - p_2) \quad (7)$$

Where, k is the valve opening coefficient.

As shown in Equation (7), k is increased from 25% to 100% and mass flow rate is increased as well.

Model of a supply manifold

A supply manifold supplies air from the compressor outlet to the cathode of the fuel cell stack. The Inlet air flow rate to the cathode side is determined by the pressure difference between the compressor exit and cathode inlet of fuel cell stack. Since the pressure difference between the supply manifold and the cathode is relatively small (7), the nozzle equation of supply manifold is determined by a linearized form.

$$W_{sm,out} = \alpha k_{sm,out}(p_{sm} - p_{ca}) \quad (8)$$

Where, is reference coefficient, $\alpha = 3.6294 \times 10^{-6}$

The mass flow rate in the supply manifold is calculated by conservation of the mass equation and the ideal gas law.

$$\frac{dm_{sm}}{dt} = (W_{cp} - W_{sm,out}) \quad (9)$$

$$\frac{dp_{sm}}{dt} = \frac{\gamma R_a}{V_{sm}}(W_{cp} T_{cp,out} - W_{sm,out} T_{sm}) \quad (10)$$

Model of cathode air flow rate

A flow-passing cathode of a fuel cell stack enters the return manifold. The air flow rate can be considered as a cathode air flow rate and the air flow rate is supplied by the pressure difference between the cathode downstream and the return manifold. Since the pressure difference between the supply manifold and the cathode is relatively small, the nozzle equation of the cathode outlet flow rate is determined by a linearized form.

$$W_{ca,out} = \beta k_{ca,out}(p_{ca} - p) \quad (11)$$

Where, is reference coefficient, $\beta = 2.1776 \times 10^{-6}$

The temperature of the air leaving the stack is relatively low when compared to the air leaving the compressor. Therefore, the mass conservation principle is used to calculate mass flow rate in the return manifold.

$$\frac{dm_{rm}}{dt} = (W_{ca,out} - W_{rm,out}) \quad (12)$$

$$\frac{dp_{rm}}{dt} = \frac{\gamma R_a}{V_{rm}}(W_{ca,out} - W_{rm,out}) \quad (13)$$

Model of the return manifold

As shown in Fig. 1, if the pressure difference is large, a nonlinear form is used to calculate the mass flow rate.

Therefore, Because of the pressure drop between the return manifold and the atmospheric is relatively large, and the return manifold out flow rate is designed by nonlinear nozzle equations. (11)

$$\dot{W}_{rm,out} = \frac{C_{D,rm} A_{T,rm} p_{rm}}{(RT_{rm})^{1/2}} \left(\frac{p_{atm}}{p_{rm}} \right)^{1/\gamma} \left\{ \frac{2\gamma}{\gamma-1} \left[1 - \left(\frac{p_{atm}}{p_{rm}} \right)^{(\gamma-1)/\gamma} \right] \right\}^{1/2} \quad \frac{p_{atm}}{p_{rm}} > \frac{2}{\gamma+1}^{\gamma/(\gamma-1)} \quad (14)$$

$$\dot{W}_{rm,out} = \frac{C_{D,rm} A_{T,rm} p_{rm}}{(RT_{rm})^{1/2}} \gamma^{1/2} \left(\frac{2}{\gamma+1} \right)^{\gamma+1/2(\gamma-1)} \quad \frac{p_{atm}}{p_{rm}} < \frac{2}{\gamma+1}^{\gamma/(\gamma-1)} \quad (15)$$

The outlet mass flow rate is a function of the manifold pressure, p_{rm} , and the pressure downstream from the manifold p_{atm}. The valve opening area, A_T, is constant or variable, but this study set is constant because $k_{sm,out}$ *and* $k_{ca,out}$ are variables to control surge.

System integration with an automotive fuel cell stack

In this study, a fuel cell system is composed of a compressor, manifolds (supply and return), a humidifier, a hydrogen supply model, a fuel cell stack and a cooling system. Referenced from Han et al. (11) and Yu et al (11), a fuel cell mode was constructed to model species mass transfer and an energy conservation equation. Therefore, the fuel cell voltage and power is calculated from

$$V_{FC} = V_{Nern} - J \cdot R(\lambda)_{mem} - \eta \quad (16)$$

$$P_{cv} = V_{FC} \cdot J \cdot n_{FC} \quad (17)$$

Dynamic simulation

A typical vehicular fuel cell system was used in this study because transient response is very important in the vehicle and surge control is very important during various operating

Table 1 Compressor nozzle opening area with cases

Case	Nozzle opening area percent(K_{sm})	Nozzle opening area percent(K_{ca})
1	25%	25%
2	25%	50%
3	25%	75%
4	25%	100%
5	50%	25%
6	50%	50%
7	50%	75%
8	50%	100%
9	75%	25%
10	75%	50%

11	75%	75%
12	75%	100%
13	100%	25%
14	100%	50%
15	100%	75%
16	100%	100%

Conditions. The input load profiles were selected to create the surge phenomenon and to control surge. The detailed parameter is shown in Table 1 below.

Load profiles

The load profile and nozzle opening coefficient are shown in Figure 2. k_{sm} and k_{ca} are CCV and TCV, respectively. The use of CCV and TCV is necessary to stabilize the compressor under various operating conditions and to extend the compressor's stable range. Therefore CCV and TCV have the advantages of the ability to control surge. so, surge can be actively controlled. Furthermore, in this study, k_{sm} and k_{ca} were changed from 25% to 100%, respectively.

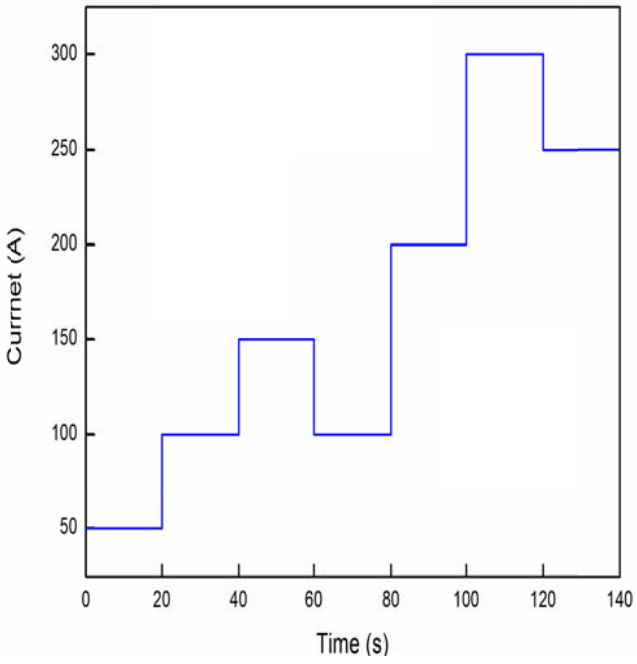

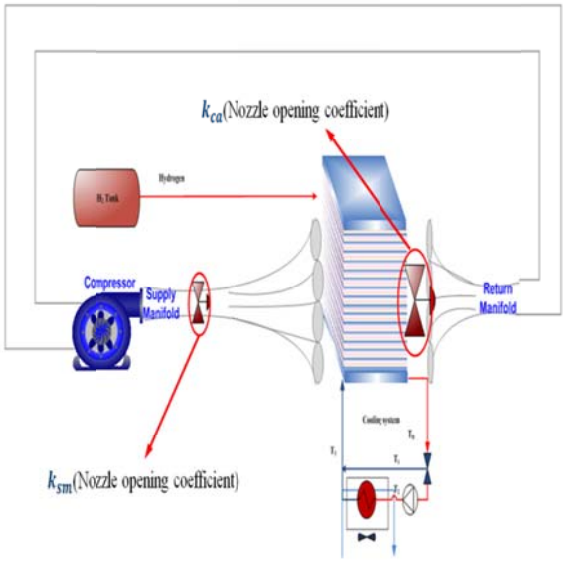

Figure 2 Load pattern and nozzle opening coefficient

RESULTS AND DISCUSSION

Transient response of the compressor on the trajectory of the compressor map

Figure 3 shows the air flow versus pressure ratio trajectory under a given load pattern. The valve of the supply manifold regulates flow such that the nozzle coefficient k_{sm} is a fixed constant. At this condition, the valve of the cathode exit is varied such that nozzle coefficient k_{ca} at the exit manifold changes. The result shows that the surge can be detected over some load conditions. The air flow rate is located outside of the surge line which implies that the surge can be detected. This is because the compressor cannot provide proper pressure rise to overcome the pressure loss through the system. As a result, the low mass flow rate of air is not properly delivered to the cathode side of the fuel cell stack. As the exit valve of cathode is fully opened, it is observed that the system operates outside the surge margin.

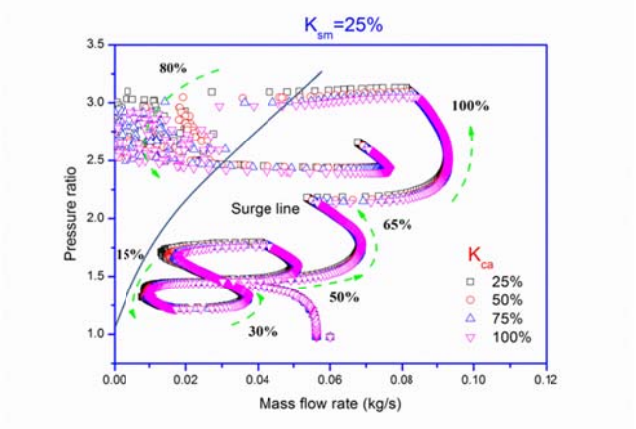

Figure 3 Compressor performance curve (K_{sm}=25%)

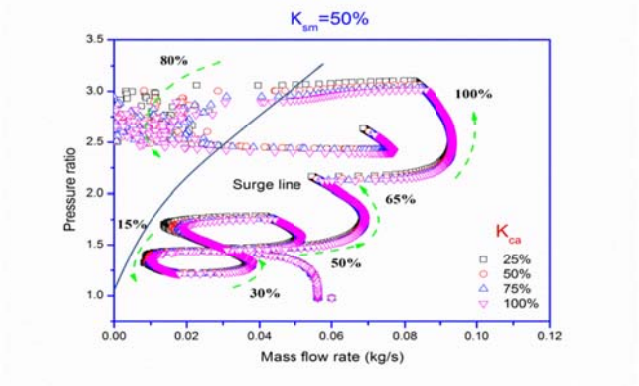

Figure 4 Compressor performance curve (K_{sm}=50%).

Figure 4 shows the compressor performance map that when the supply manifold nozzle is 50% opening. You can see that the performance curve is formed outside the surge line at all regions. When the supply manifold nozzle is 50% open, the air flow rate does not pass the stack at all regions. So, pressure ratio oscillation occurs. Therefore, the nozzle opening area from 80% to 100%, it is necessary to open the cathode manifold control valve 25%.

When the supply manifold nozzle coefficient is 75%open, you can see that the performance curve is formed outside the surge line at 25% in figure5. When the cathode nozzle coefficient is lower or equal to the supply nozzle coefficient, the air flow rate does not pass the stack. Therefore, the pressure ration oscillation occurs. Therefore, the nozzle opening area from 80% to 100%, it is necessary to open the cathode manifold control valve 25%

Next, when the supply manifold nozzle coefficient opens at 100%, you can see that the performance curve is formed outside the sure line at 25% and 50% in the figure 6 because the air flow rate through the supply manifold does not pass the cathode manifold due to a small opening area. In contrast, when k_{sm} is 100% and k_{ca} is 75% and 100%, the surge phenomenon does not occur because pressure loss does not exist at the cathode manifold outlet. Therefore, the nozzle opening area from 80% to 100%, it is necessary to open the cathode manifold control valve 50%.

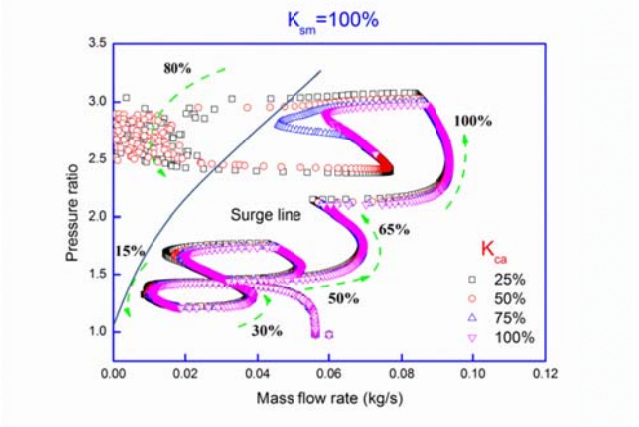

Figure 6 Compressor performance curve (K_{sm}=100%).

Control strategy to avoid surge

Figure7, 8, and 9 shows how much valve opening area is required to avoid the surge area from the compressor system. Figure 7 shows the changed supply manifold nozzle coefficient to 100% from 25%. Figure 8 shows the changed return manifold nozzle coefficient to 100% from 25%. As can be seen in the Fig.7 and Fig.8, when the system is operated around 80%, surge occurs. Thus, the compressor efficiency is very low. Also, Figure.9 makes it clear that k_{sm} and k_{ca} are dramatically increased at a high nozzle coefficient. Thus, when the system is operated at around 80%, the k_{sm} and k_{ca} nozzle coefficients have to open over 75%.

As shown in Table 3, when the current is 15%, k_{sm} and k_{ca} set up case 16 with high efficiency. Therefore, when the system is operated from 15% to 30%, the control point is set as case 16. When the load is between 50% and 100%, the surge phenomenon does not occur. So, the k_{sm} and k_{ca} set up case 1 with good compressor efficiency. Therefore, when the system is operated from 50 to 65%, the control point is set as case 1. Also, when the system operates at 80%, we can see the surge phenomenon which that occurs in almost every case. Also, the surge phenomenon section has much lower compressor efficiency. Thus, as shown in Figure 9, k_{sm} and k_{ca} is set as case 16.

Table 2 Compressor nozzle opening area with cases

Case	Nozzle opening area percent(k_{sm})	Nozzle opening area percent(k_{ca})
1	25%	25%
2	25%	50%
3	25%	75%
4	25%	100%
5	50%	25%
6	50%	50%
7	50%	75%
8	50%	100%
9	75%	25%
10	75%	50%
11	75%	75%
12	75%	100%
13	100%	25%
14	100%	50%
15	100%	75%
16	100%	100%

Table 3 Compressor efficiency for current

Case	$\eta_{I=15\%}$	$\eta_{I=30\%}$	$\eta_{I=50\%}$	$\eta_{I=65\%}$	$\eta_{I=80\%}$	$\eta_{I=100\%}$
1	75.7%	77.4%	78.9%	78.6%	29.2%	76.1%
2	76.1%	77.8%	78.9%	78.6%	30.0%	76.2%
3	76.4%	78.1%	78.9%	78.6%	38.4%	76.0%
4	76.1%	78.3%	78.9%	78.6%	41.6%	75.9%
5	75.9%	77.6%	78.9%	78.6%	30.5%	76.2%
6	76.3%	78.1%	78.9%	78.6%	35.4%	76.0%
7	76.7%	78.4%	78.9%	78.5%	35%	75.7%
8	77.0%	78.5%	78.9%	78.4%	42.0%	75.5%
9	76.0%	77.8%	78.9%	78.6%	32.1%	76.2%
10	76.5%	78.3%	78.9%	78.5%	38.8%	75.8%

11	76.9%	78.5%	78.9%	78.4%	39.6%	75.5%
12	77.2%	78.5%	78.9%	78.3%	75.7%	75.3%
13	76.1%	77.9%	78.9%	78.6%	33.6%	76.1%
14	76.7%	78.4%	78.9%	78.5%	40.3%	75.7%
15	77.1%	78.5%	78.9%	78.3%	71.0%	75.4%
16	77.4%	78.6%	78.9%	78.2%	76.7%	75.0%

Therefore, simulations show that this surge phenomenon can be avoided by opening the area of CCV to over 75%. In contrast, even if TCV is fully open, surge control can be limited at opening areas of CCV below 75%

Also, the surge phenomenon does not occur in an opening area of 75% only if TCV is fully open and if the opening area of CCV is 100%, and the surge phenomenon can be controlled only if TCV opens over 75%.

Comparison of energy saving

The percentage of net energy savings of the compressor system is determined by the equation blow. The net energy of the compressor system is:

$$E_{tot} = \int P_{net}\, dt \tag{18}$$

The gain of net energy of the compressor system is as follows:

$$\%E_{net,save} = \frac{E_{net,non-surge} - E_{net,surge}}{E_{net,surge}} \times 100 \tag{19}$$

The calculation shows that $k_{sm}, k_{ca} = 100\%$ and gained 0.8% net energy savings for the compressor system.

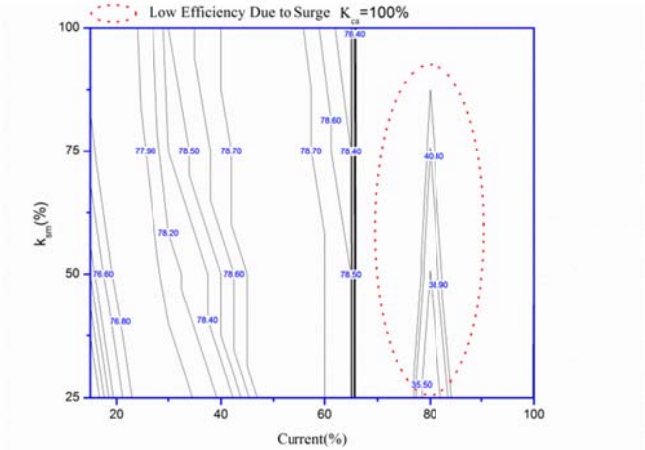

Figure7 Efficiency over supply manifold nozzle coefficient. (k_{ca}=100%)

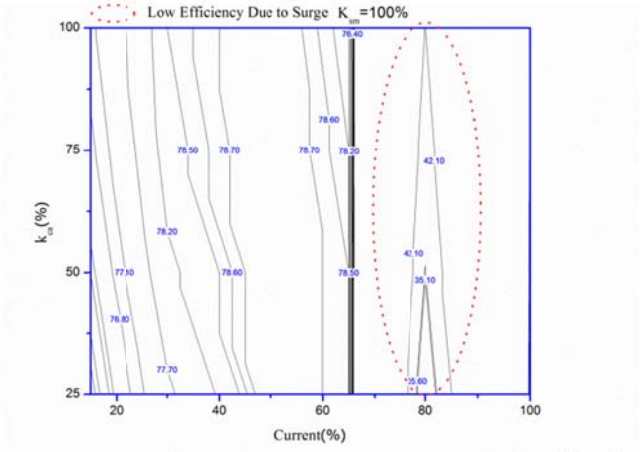

Figure8 Efficiency over return manifold nozzle coefficient. (k_{sm}=100%)

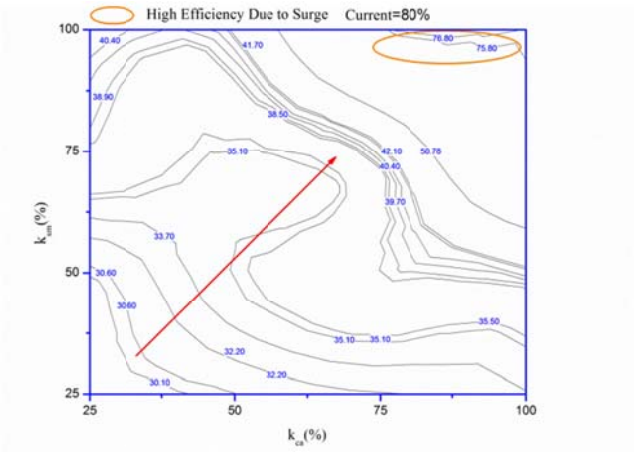

Figure9 Contour plot of efficiency (current=80%)

Control strategy to operate the system at optimal efficiency without surge

Fig. 10 shows the compressor performance curve trajectories during the load pattern under control logic.

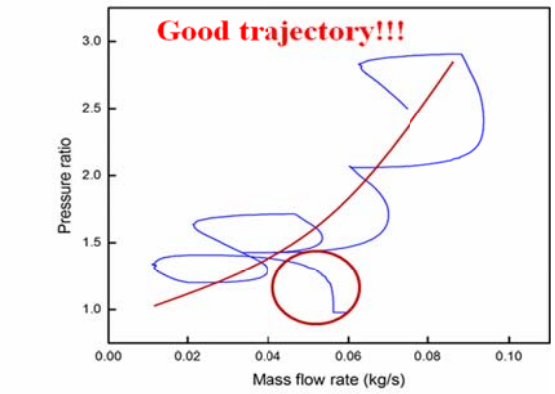

Figure 10 Compressor transient response on compressor map under control logic.

The performance curve is in good agreement with that of the compressor map. If the control valve is installed downstream of the cathode manifold good trajectory is achieved.

Therefore, the combination of CCV and TCV is needed to control surge. Also, when the load is 80%, the surge phenomenon can be controlled only if CCV opens over 75% and TCV opens at least over 75%.

CONCLUSION

In this study, a dynamic simulation of an automotive fuel cell system was developed to understand compressor surge over load changes.

1. The surge effect can be effectively reduced by increasing the k_{ca} nozzle coefficient, but the nozzle of the compressor downstream does not affect the avoidance of surge at 80%.

2. When the system operates at 15% and 30%, case 16 shows the highest efficiencies of 77.4% and 78.6%, respectively. As the system operate at 50% and 65%, case 1 results in high efficiencies 78.9% and 78.6%, respectively. And at 80% and 100%, case 16 results in high efficiencies 76.7% and 75.0%, respectively.

3. The calculation shows that $k_{sm}, k_{ca} = 100\%$ and gained 0.8% net energy savings for the compressor system.

4. Accordingly, the active control of a combination of CCV and TCV is necessary to achieve active surge reduction as well as efficient operation.

ACKNOWLEDGMENTS

This research was supported under a Basic Science Research Program (grant number: 2010-0021304) and Human Resource Training Project for Regional Innovation (Project No. 201206A0106312010100) through the National Research Foundation of Korea(NRF), funded by the Ministry of Education.

REFERENCES

[1] http://www.fuelfromthewater.com/transportation.htm

[2] Greitzer, E.M., 1976, "Surge and Rotating Stall in Axial Flow Compressors, Part Ⅰ: Theoretical Compression System Model," ASME Journal of Engineering for Power, Vol. 98, pp. 190~198.

[3] Greitzer, E.M., 1976, "Surge and Rotating Stall in Axial Flow Compressors, Part Ⅱ: Experimental Results and Comparison With Theory," ASME Journal of Engineering for Power, Vol. 98, pp. 199~211.

[4] Moore, G. K. and Greitzer, E.M., 1986, "A theory of post-stall transient in axial compression system: Part Ⅰ - development of equations," ASME Journal of Engineering for Gas Turbines and Power, Vol. 108, pp. 68~76.

[5] Hansen, K.E., 1981, "Experimental and Theoretical Study of Surge in a Small Centrifugal Compressor," ASME Journal of Fluids Engineering, Vol. 103, pp. 391~395.

[6] Shelhata, R.S., Abdullah, H.A. and Areed, F.F.G., 2009, "Variable structure surge control for constant speed centrifugal compressors," Control Engineering Practice, Vol 17, pp. 815~833.

[7] Galindo, J., Serrano, J.R., Climent, H. and Tiseira, A., 2008, " Experiments and modelling of surge in small centrifugal compressor for automotive engines," Experimental Thermal and Fluid Science, Vol. 32, pp. 818~826.

[8] Tirnovan, R., Miraoui, A. and Giurgea, S., 2007, Modeling and Analysis of a High Pressure Operating Fuel Cell Hydrogen/air system, Proceedings of IEEE.

[9] Heywood, J.B., 1998, Internal Combustion Engine Fundamentals. McGraw-Hill, New York, pp. 220~226

[10] Pukrushpan, J., Stefanopoulou, A. G. and Peng, H., 2004, Control of Fuel Cell Power Systems, Springer, London, First Edition, pp. 15~20.

[11] Han, J.Y., Lee, K.H. and Yu, S.S., 2012, Dynamic Modeling of Cooling System Thermal Management for Automotive PEMFC Application, Trans of the KSME(B), Vol. 36(12) , pp. 1185~1192.

[12] Yu, S.S., Kim, H.S., Lee, S.M., Lee, Y.D. and Ahn, K.Y., 2007, Thermal Management of Proton Exchange Membrane Fuel Cell, Trans. of the Korean Hydrogen and New Energy Society, Vol. 18 , No. 3, pp. 292~300.